



www.asianpubs.org

ARTICLE

Exploring 3D QSAR Study of Pyridone-Pyrimidone Derivatives as Glucokinase Activators in Treatment of Diabetes Mellitus by using CoMFA Method

Priyanka N. Chhajed[✉] and Ravindra B. Patil

Asian Journal of Organic & Medicinal Chemistry

Volume: 7

Year: 2022

Issue: 1

Month: January–March

pp: 42–54

DOI: <https://doi.org/10.14233/ajomc.2022.AJOMC-P360>

Received: 14 January 2022

Accepted: 14 February 2022

Published: 5 April 2022

Author affiliations:

DCS's Annasaheb Ramesh Ajmera College of Pharmacy, Nagaon-424005, India

[✉]To whom correspondence to be addressed:

E-mail: Chhajedpriyanka123@gmail.com

Available online at: <http://ajomc.asianpubs.org>

ABSTRACT

In this work, we have performed 3D QSAR study of reported pyridone-pyrimidone derivatives. CoMFA was applied to generate 3D QSAR models. Total eight QSAR models were generated. Model 2 was close to standard set criteria. Effect of steric and electrostatic substituents on biological activity was observed on contour maps. This study will be helpful for future researchers in designing new pyridine-pyrimidone derivatives.

KEYWORDS

Glucokinase, Pyridone-Pyrimidone, 3D QSAR, Diabetes mellitus.

INTRODUCTION

Glucose balance is very important to mammalian survival. Glucose imbalance can lead to various disorders, like type 2 diabetes mellitus [1,2]. Type 2 diabetes mellitus has become more prevalent disease day-by-day. Many therapies available in the market, but are associated with some side effects. As a result, the quest for new antidiabetic medications continues. In glucose homeostasis, glucokinase (hexokinase IV) plays a distinctive role. Glucokinase is a monomeric enzyme that converts D-glucose into glucose-6-phosphate in the presence of ATP. The drugs which activate glucokinase enzyme are known as glucokinase activators [3]. Variety of glucokinase activators like benzamide derivatives, phenyl acetamide derivatives, sulfonamides, quinazolines and benzimidazole derivatives have been reported till date [2-7]. Pyridine derivatives have also been reported as glucokinase activators [8,9].

In this work, 3D QSAR study of reported pyridone-pyrimidone derivatives is performed. We have used webserver <https://www.3d-qsar.com/> [10]. There are several web applications available in this server [11] like (1) Py-MolEdit, which allows for the compilation of the data set by either uploading a list of molecules in any open babel recognized format or drawing directly in a java script molecular editor; (2) Py-ConfSerch, which contains different conformational analysis engines to generate conformational ensembles for each dataset molecule; (3) Py-Align, which allows for molecular alignment on up to 16 pre-defined different templates using automatic molecular alignment software; and (4) Py-CoMFA,

which works in the same way as the original CoMFA software for creating and validating 3-D QSAR models [11,12].

EXPERIMENTAL

Collection and preparation of ligands (dataset): Total 28 pyridone, pyrimidone-based series of glucokinase activators, reported in the literature [9], were used for 3D QSAR study. Structural data for the dataset was obtained from the Pubchem database in .sdf format. All ligands were prepared using Biovia Discovery studio software 2020.

3D QSAR studies

Generation of CoMFA-based QSAR models [8-10]: We have used webserver <https://www.3d-qsar.com/>. We have used CoMFA to develop QSAR models [10]. The shape of a molecule is used by CoMFA [4]. Molecular interaction fields were calculated at each grid point using a probe atom during the method, which describes molecules that have virtually united into a cuboid grid. In the typical CoMFA, only two potentials are used: steric (STE) and electrostatic (ES) (ELE). PLS is used to identify the quantitative effect of physico-chemical characteristics of compounds on their pharmacological activity [4] and the molecular interaction Fields are linearly correlated with the training set biological activity data. We took 28 pyridone, pyrimidone-based series of glucokinase activators as a data set, categorized them into training and test set. Out of 28 molecules, 20 were categorized into training set and 8 molecules

were into test set. Table-1 shows structures of pyridone-pyrimidone derivatives reported in literature along with actual EC_{50} and pEC_{50} values. Test set compounds are shown with asterisk* in Table-1. The molecular interaction fields between probe atoms and molecules were calculated using aligned molecules in a grid box [4]. Fig. 1 shows the flowchart of 3D QSAR workflow.

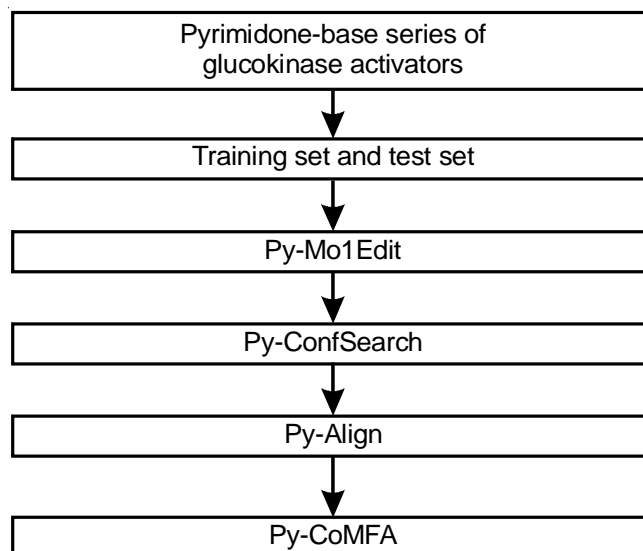


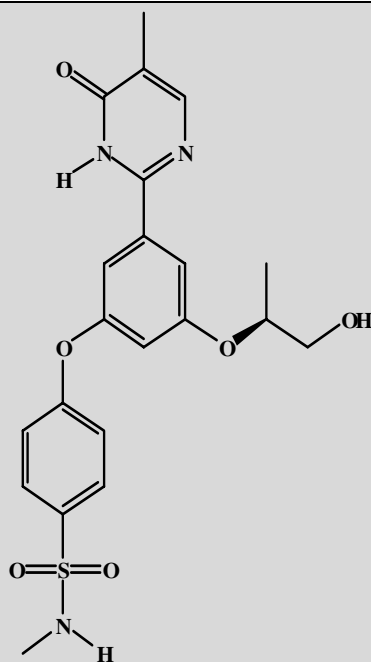
Fig. 1. 3D QSAR modeling workflow as given on www.3d-qsar.com

TABLE-1
STRUCTURES OF PYRIDONE-PYRIMIDONE DERIVATIVES REPORTED IN
LITERATURE ALONG WITH ACTUAL EC_{50} VALUES ACTUAL pEC_{50}

| S. No. | Compound Pubchem CID | Structure | EC_{50} (nM) | Actual/experimental pEC_{50} |
|--------|----------------------|-----------|----------------|--------------------------------|
| 1 | 71627422* | | 2000 | 5.70 |
| 2 | 54767120 | | 940 | 6.03 |

3

54765716

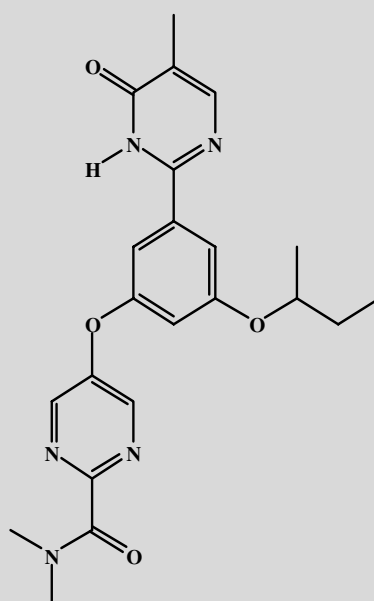


110

6.96

4

54767787

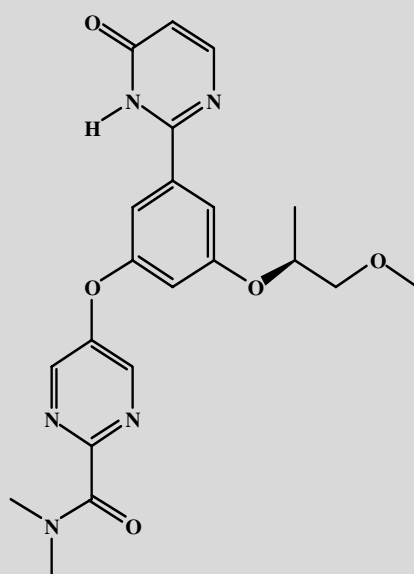


170

6.77

5

54766497

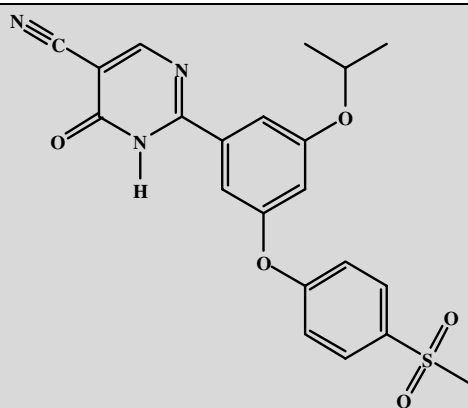


1000

6.00

6

67996937*

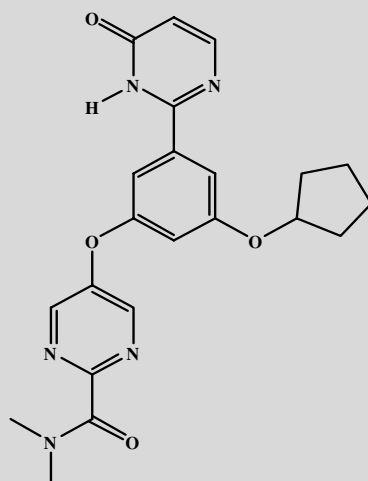


9200

5.04

7

54766199*

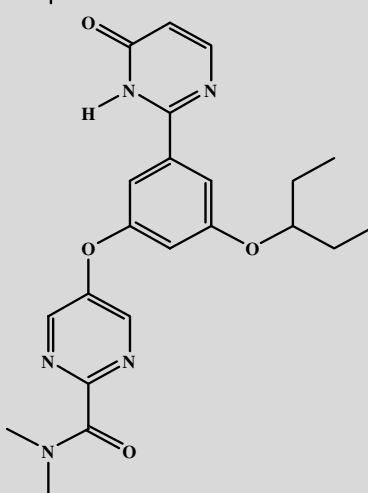


440

6.36

8

54766500

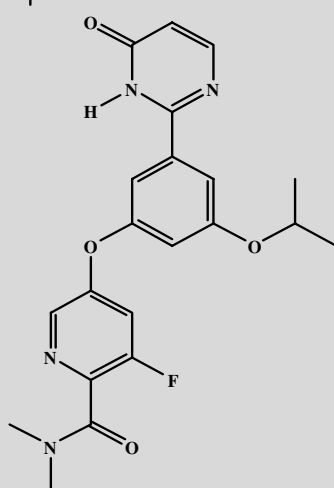


230

6.64

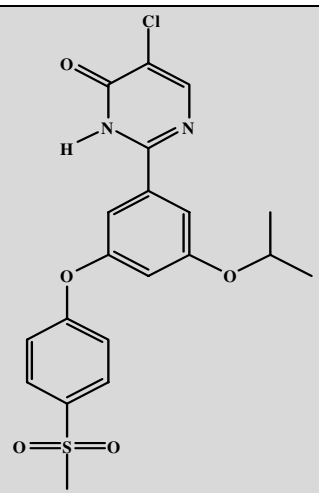
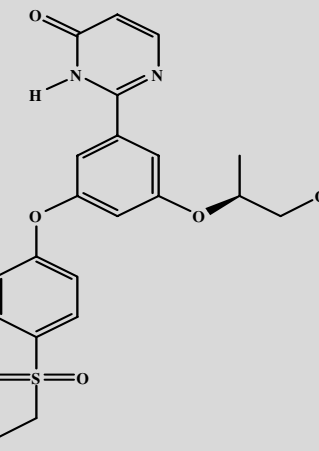
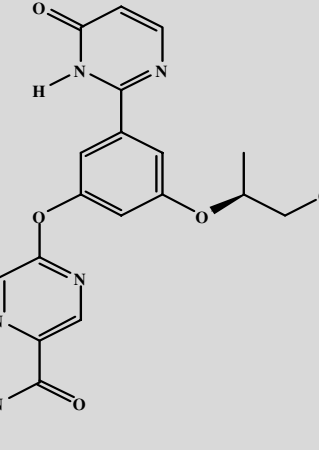
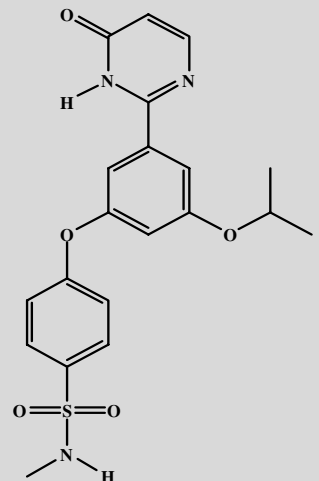
9

54767786



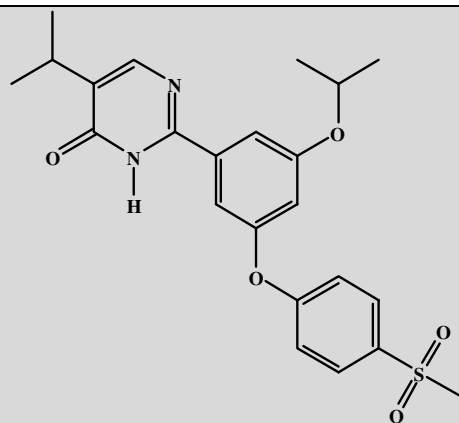
230

6.64

| | | | | |
|----|-----------|---|------|------|
| 10 | 54767119* |  | 7500 | 5.12 |
| 11 | 54767447 |  | 150 | 6.82 |
| 12 | 54766195 |  | 200 | 6.70 |
| 13 | 54767784 |  | 1400 | 5.85 |

14

54766044

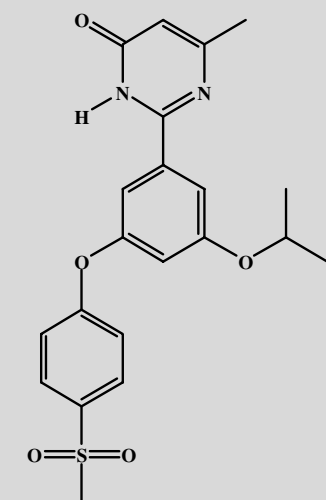


590

6.23

15

136239454

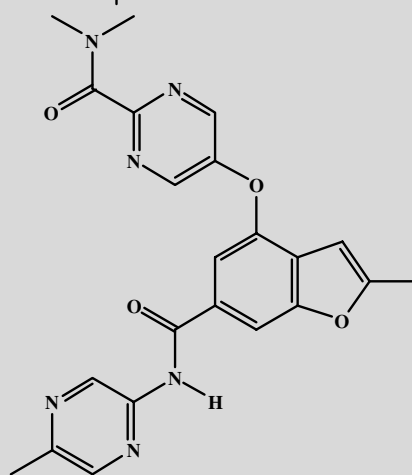


10300

4.99

16

46916694

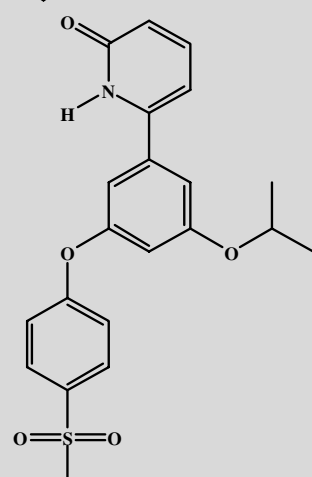


190

6.72

17

71813336



740

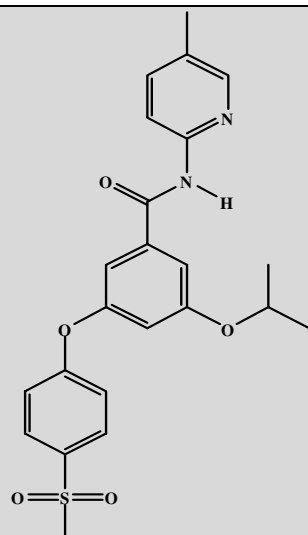
6.13

18

73350645

110

6.96

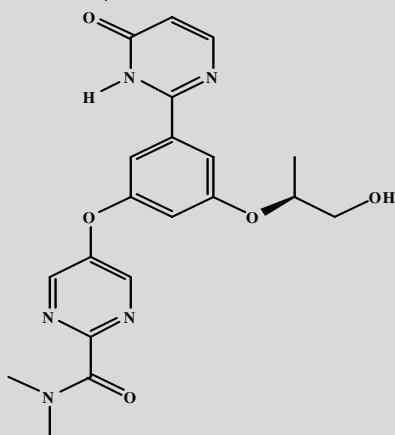


19

54765880

1100

5.96

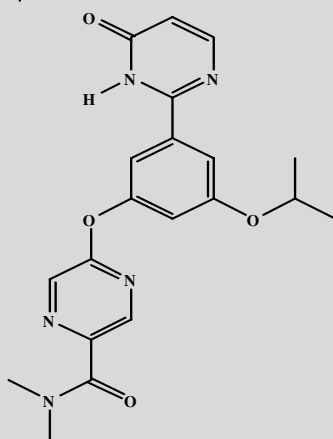


20

54767782*

500

6.30

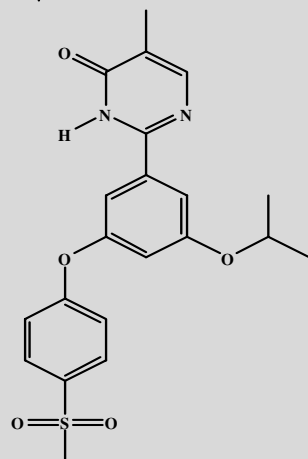


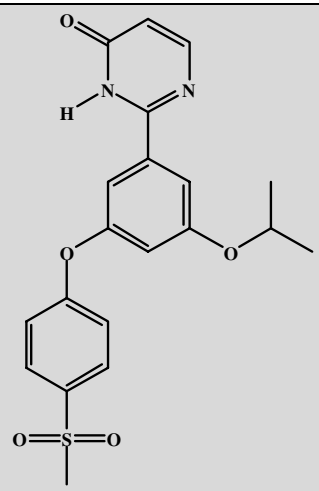
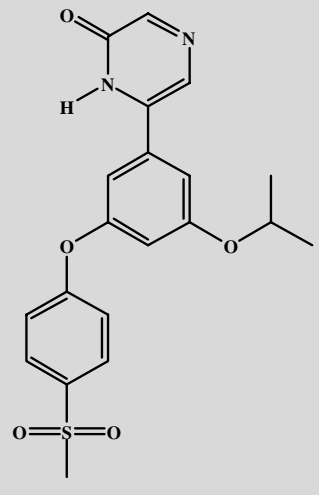
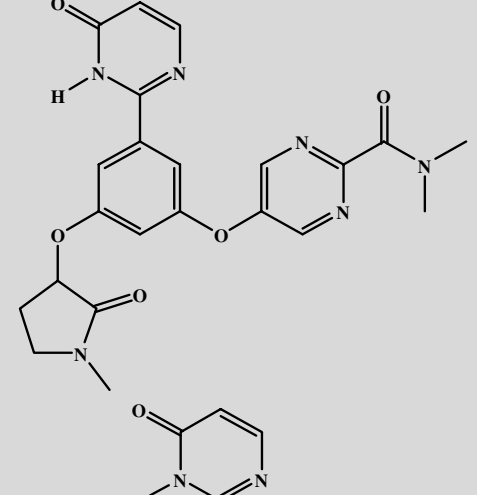
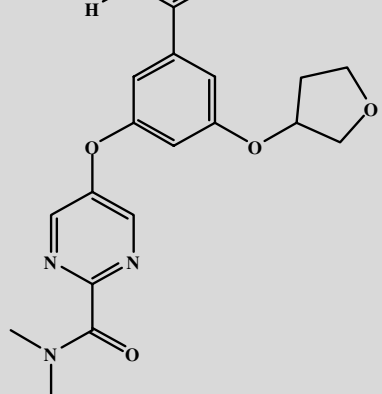
21

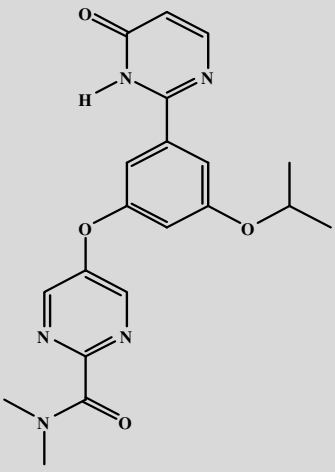
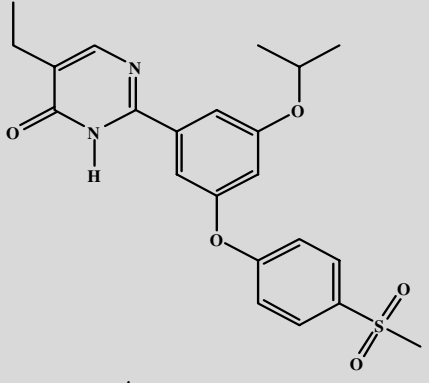
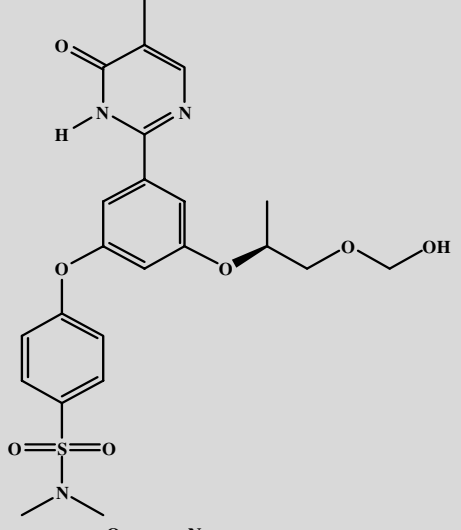
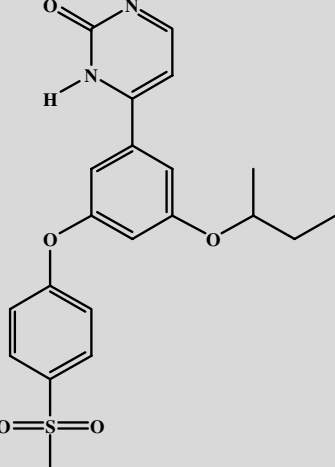
54767116

200

6.70



| | | | | |
|----|-----------|--|-------|------|
| 22 | 54767117 |  | 830 | 6.08 |
| 23 | 71813669* |  | 23000 | 4.64 |
| 24 | 71814304* |  | 3800 | 5.42 |
| 25 | 67996575* |  | 7500 | 5.12 |

| | | | | |
|----|----------|--|--------|----------|
| 26 | 54767610 |  | 850 | 6.07 |
| 27 | 54767118 |  | 70 | 7.15 |
| 28 | 54765712 |  | 90 | 7.05 |
| 29 | 71813504 |  | 100000 | Not used |

RESULTS AND DISCUSSION

QSAR results of the 28 pyridone, pyrimidone-based series of glucokinase activators: For QSAR study, biological activities reported in the literature as EC_{50} (nM) were converted to pEC_{50} . To determine the predicted pEC_{50} value in the 3D-QSAR, The whole dataset was divided randomly into a test set and training sets in 3:7 ratio [10]. There were 28 molecules in total, 20 were used as a training set and 08 as test set. Test set molecules are shown with asterisk*. Training set compounds were utilized to construct the CoMFA based QSAR models and test set molecules were utilized to validate the models. For evaluation of QSAR models, parameters like squared cross-validation coefficient (q^2), squared non-cross-validation coefficient (r^2), error fit, error CV and predictive r^2 were considered [4]. We got 8 models, among them; model no. 2 had shown the better value of q^2 for both steric and electrostatic as -0.764. Model 2 showed r^2 value as 0.943 (standard value near to 1). Table-2 shows the results of all 8 QSAR models. Table-3 shows the results of QSAR of the training and test sets' fit. It was concluded based on this hypothesis that none of the 8 generated models met the criteria set forth. But, model 2 was close to standard criteria [4].

Contour map analysis: Fig. 2 shows an alignment of training set ligands. Figs. 3-5 show positive steric contour map of most potent compound, 54767118, as a template. Figs. 6-8 show negative steric contour map of most potent compound, 54767118, as a template. Figs. 9-11 show positive electrostatic contour map of most potent compound, 54767118, as a template.

| PC | Optimal PC | r^2 | SDEC | q^2 | SDEP |
|----|------------|-------|-------|--------|-------|
| 1 | | 0.724 | 0.075 | -0.834 | 0.496 |
| 2 | * | 0.943 | 0.015 | -0.764 | 0.477 |
| 3 | | 0.982 | 0.005 | -0.817 | 0.492 |
| 4 | | 0.998 | 0.001 | -0.778 | 0.481 |
| 5 | | 0.999 | 0 | -0.753 | 0.474 |
| 6 | | 1 | 0 | -0.761 | 0.477 |
| 7 | | 1 | 0 | -0.757 | 0.475 |
| 8 | | 1 | 0 | -0.755 | 0.475 |

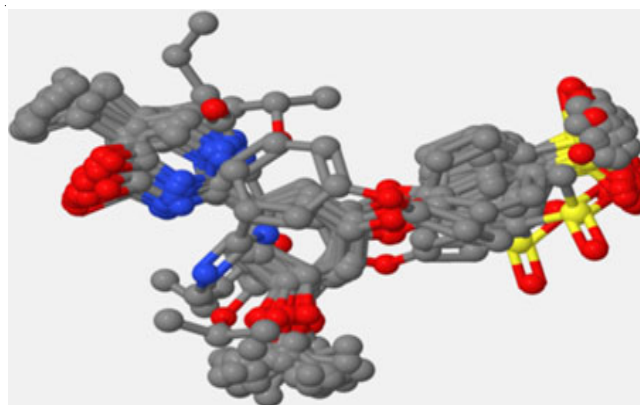


Fig. 2. Alignment of training set molecules

Figs. 12-14 show negative electrostatic contour map most potent compound, 54767118, as a template.

TABLE-3
ACTUAL pIC_{50} , PREDICTED pIC_{50} AND RESIDUAL VALUES OF GENERATED CoMFA
MODEL (CoMFA QSAR STATISTICS FOR BOTH STERIC AND ELECTROSTATIC)

| S. No. | Name (Pubchem CID) | Exp | Fit/Pred | Err Fit/Pred | CV | Err CV | Mol Set |
|--------|--------------------|-------|----------|--------------|-------|--------|--------------|
| 1 | 46916694 | 6.721 | 6.892 | -0.17 | 6.267 | 0.454 | Training set |
| 2 | 54765712 | 7.046 | 6.897 | 0.149 | 5.549 | 1.497 | Training set |
| 3 | 54765716 | 6.959 | 6.803 | 0.155 | 6.458 | 0.5 | Training set |
| 4 | 54765880 | 5.959 | 5.867 | 0.092 | 6.338 | -0.38 | Training set |
| 5 | 54766044 | 6.229 | 6.374 | -0.144 | 6.802 | -0.573 | Training set |
| 6 | 54766195 | 6.699 | 6.844 | -0.145 | 6.603 | 0.096 | Training set |
| 7 | 54766497 | 6 | 5.922 | 0.078 | 6.331 | -0.331 | Training set |
| 8 | 54766500 | 6.638 | 6.893 | -0.255 | 6.427 | 0.211 | Training set |
| 9 | 54767116 | 6.699 | 6.542 | 0.157 | 6.198 | 0.501 | Training set |
| 10 | 54767117 | 6.081 | 6.152 | -0.071 | 6.571 | -0.49 | Training set |
| 11 | 54767118 | 7.155 | 7.06 | 0.095 | 6.351 | 0.804 | Training set |
| 12 | 54767120 | 6.027 | 5.984 | 0.043 | 6.296 | -0.269 | Training set |
| 13 | 54767447 | 6.824 | 6.85 | -0.026 | 6.449 | 0.374 | Training set |
| 14 | 54767610 | 6.071 | 5.957 | 0.113 | 6.331 | -0.261 | Training set |
| 15 | 54767784 | 5.854 | 5.904 | -0.05 | 6.634 | -0.78 | Training set |
| 16 | 54767786 | 6.638 | 6.68 | -0.041 | 6.583 | 0.055 | Training set |
| 17 | 54767787 | 6.77 | 6.812 | -0.042 | 6.479 | 0.291 | Training set |
| 18 | 71813336 | 6.131 | 6.185 | -0.055 | 6.658 | -0.528 | Training set |
| 19 | 73350645 | 6.959 | 6.754 | 0.205 | 6.241 | 0.717 | Training set |
| 20 | 136239454 | 4.987 | 5.076 | -0.088 | 6.806 | -1.819 | Training set |
| 21 | 54766199 | 6.357 | 6.621 | -0.265 | - | - | Test set |
| 22 | 54767119 | 5.125 | 6.319 | -1.194 | - | - | Test set |
| 23 | 54767782 | 6.301 | 6.107 | 0.194 | - | - | Test set |
| 24 | 67996575 | 5.125 | 6.265 | -1.14 | - | - | Test set |
| 25 | 67996937 | 5.036 | 5.916 | -0.88 | - | - | Test set |
| 26 | 71627422 | 5.699 | 5.899 | -0.2 | - | - | Test set |
| 27 | 71813669 | 4.638 | 5.986 | -1.347 | - | - | Test set |
| 28 | 71814304 | 5.42 | 5.745 | -0.325 | - | - | Test set |

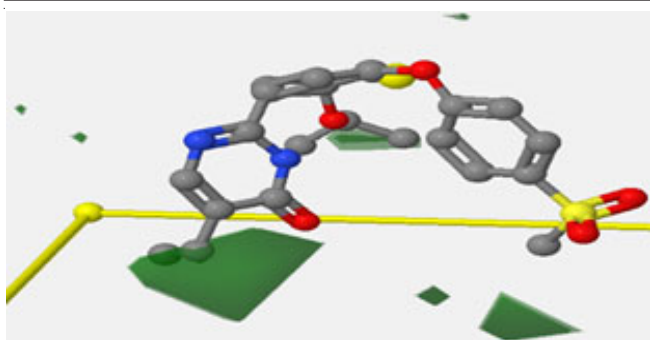


Fig. 3. Steric contour map of 54767118 for steric coefficient positive

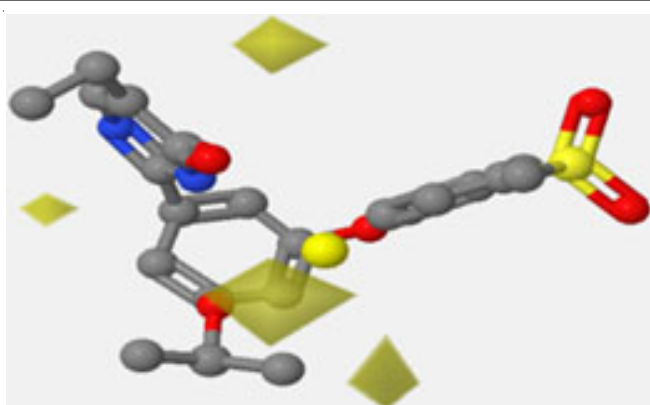


Fig. 7. Steric contour map of 54767118 for steric coefficient negative

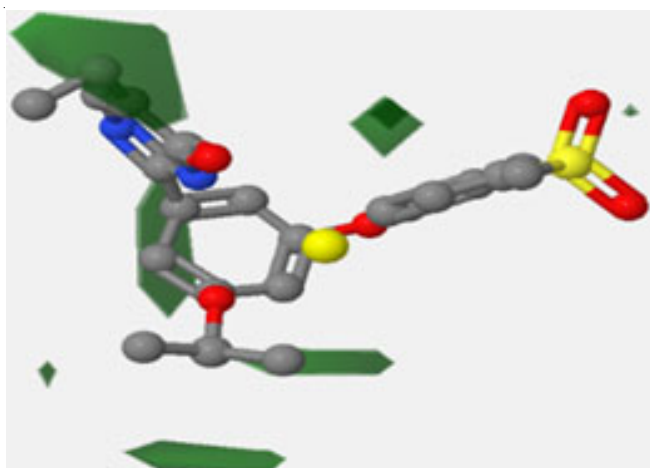


Fig. 4. Steric contour map of 54767118 for steric coefficient positive

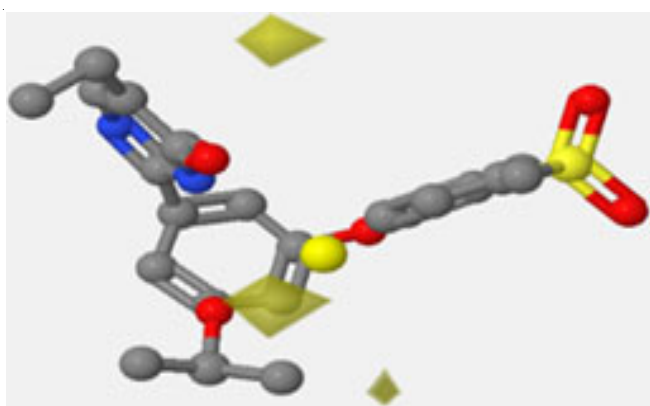


Fig. 8. Steric contour map of 54767118 for steric coefficient negative

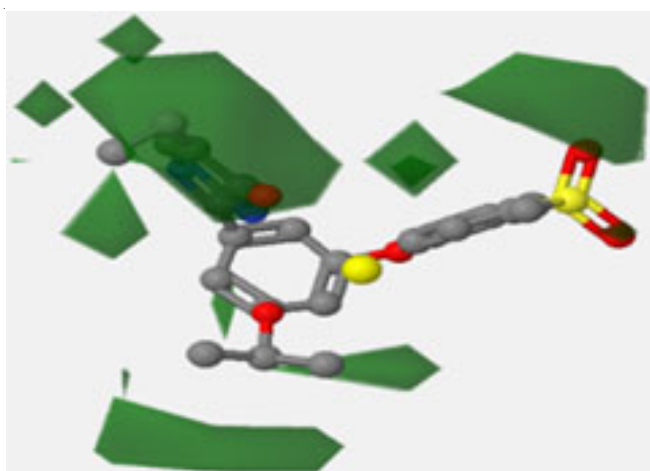


Fig. 5. Steric contour map of 54767118 for steric coefficient positive

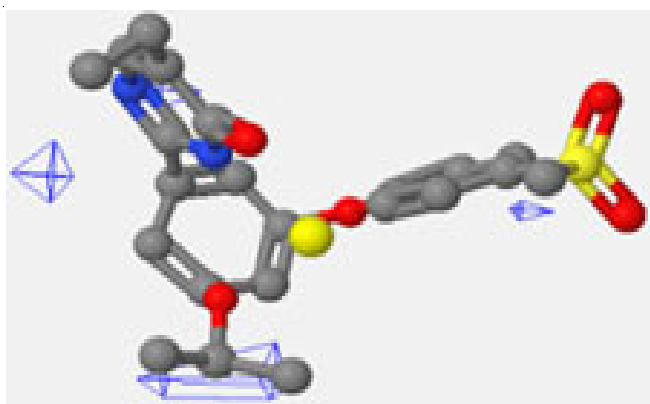


Fig. 9. Electrostatic contour map of 54767118 for electrostatic coefficient positive

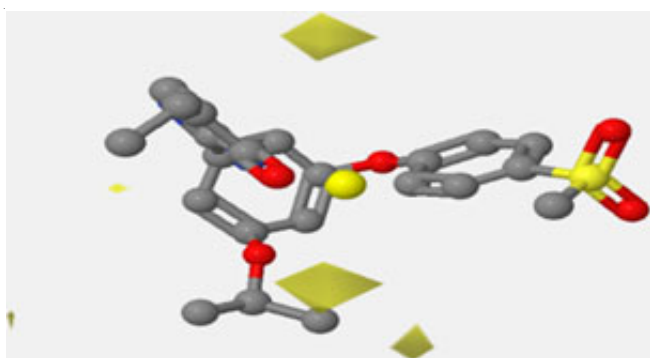


Fig. 6. Steric contour map of 54767118 for steric coefficient negative

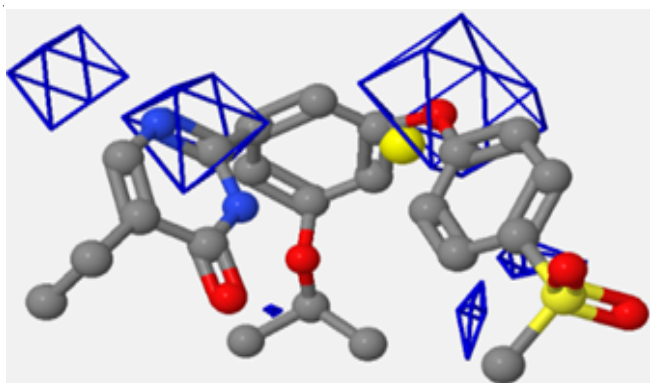


Fig. 10. Electrostatic contour map of 54767118 for electrostatic coefficient positive

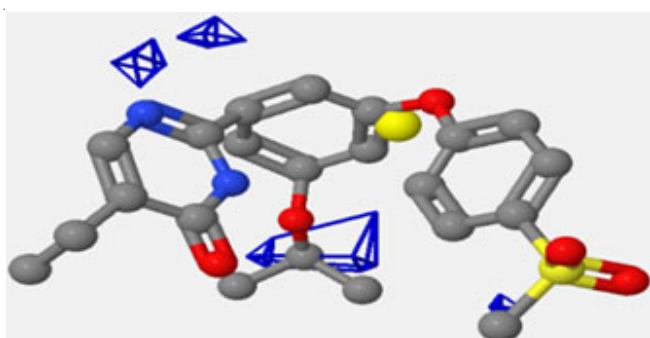


Fig. 11. Electrostatic contour map of 54767118 for electrostatic coefficient positive

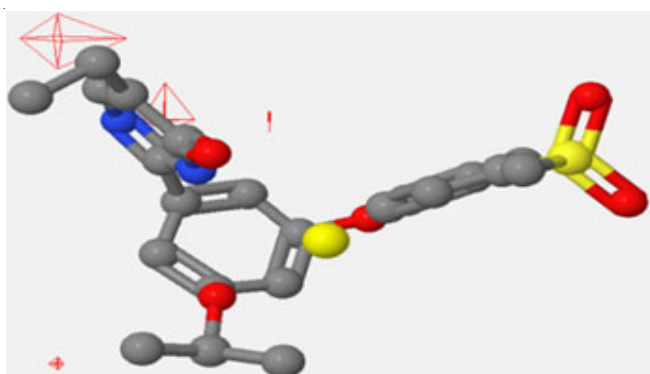


Fig. 12. Electrostatic contour map of 54767118 for electrostatic coefficient negative

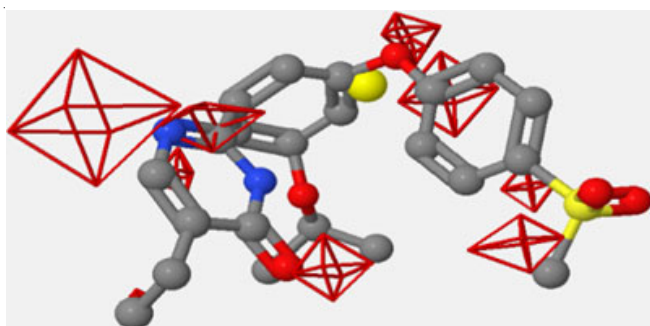


Fig. 13. Electrostatic contour map of 54767118 for electrostatic coefficient negative

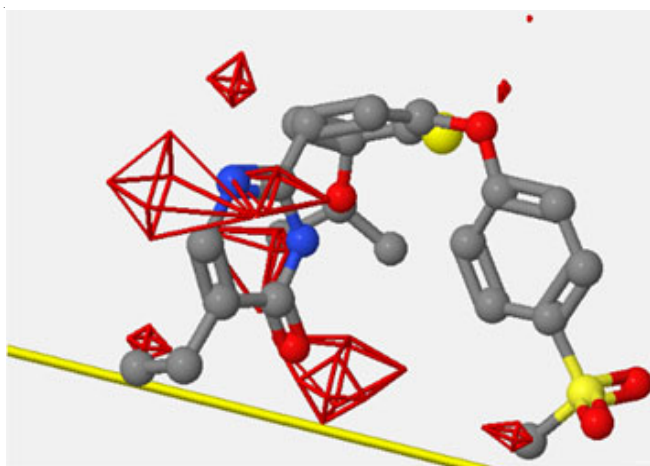


Fig. 14. Electrostatic contour map of 54767118 for electrostatic coefficient negative

Green-coloured contour shows that we can substitute steric substituents at that position [5]. In pyrimidone, at 3rd position we can substitute steric substituent, at sulphonyl group steric substituent can be added and in *ortho* aryl group, we can add steric substituent. Yellow-coloured contour shows that we cannot substitute steric substituents at that position. The phenyl ring attached to sulphonyl group cannot be substituted with steric substituents. The blue-coloured contours in CoMFA's electrostatic contour map indicate that we can substitute electropositive groups at these positions whereas large red-coloured contours indicate that electronegative groups can be substituted here. At sulphonyl group electropositive substituent can be added and in *ortho* aryl group, we can added electropositive substituent. The phenyl ring attached to sulphonyl group cannot be substituted with electronegative groups, next to oxygen attachment.

Conclusion

In current 3D QSAR study, we have used 28 pyridone-pyrimidone derivatives reported in the literature with their EC₅₀ values. All the 28 compounds were divided into training and test set molecules. 3D QSAR models were generated using www.3d-qsar.com as a webserver. CoMFA models were generated and validated by using test set molecules. Total 8 models were generated by webserver. None of them fulfilled the standard criteria given for q^2 and r^2 . But model 2 was closed to standard criteria. From the model and contour maps, we came to know about where to substitute steric and electrostatic substituents in pyrimidine structures for improved biological activities. This study will be helpful to researchers during designing of pyrimidone derivatives.

REFERENCES

1. M.A. Hossain and R. Pervin, Current Antidiabetic Drugs: Review of their Efficacy and Safety, In: Nutritional and Therapeutic Interventions for Diabetes and Metabolic Syndrome, Elsevier, Academic Press: Waltham, Ed.: 2, pp. 455–473 (2018).
2. T.O. Johnson and P.S. Humphries, Glucokinase Activators for the Treatment of Type 2 Diabetes, *Ann. Rep. Med. Chem.*, **41**, 141 (2006); [https://doi.org/10.1016/S0065-7743\(06\)41008-3](https://doi.org/10.1016/S0065-7743(06)41008-3)
3. M. Pal, Recent Advances in Glucokinase Activators for the Treatment of Type 2 Diabetes, *Drug Discov. Today*, **14**, 784 (2009); <https://doi.org/10.1016/j.drudis.2009.05.013>
4. S. Bhattacharya, V. Asati, M. Mishra, R. Das, V. Kashaw and S.K. Kashawa, Integrated Computational Approach on Sodium-Glucose Co-Transporter 2 (SGLT2) Inhibitors for the Development of Novel Antidiabetic Agents, *J. Mol. Struct.*, **1227**, 129511 (2020); <https://doi.org/10.1016/j.molstruc.2020.129511>
5. N. Charaya, D. Pandita, A.S. Grewal and V. Lather, Design, Synthesis and Biological Evaluation of Novel Thiazol-2-yl Benzamide Derivatives as Glucokinase Activators, *Comput. Biol. Chem.*, **73**, 221 (2018); <https://doi.org/10.1016/j.compbiolchem.2018.02.018>
6. Z.S. Cheruvallath, S.L. Gwaltney II, M. Sabat, M. Tang, J. Feng, H. Wang, J. Miura, P. Guntupalli, A. Jennings, D. Hosfield, B. Lee and Y. Wu, Design, Synthesis and SAR of Novel Glucokinase Activators, *Bioorg. Med. Chem. Lett.*, **23**, 2166 (2013); <https://doi.org/10.1016/j.bmcl.2013.01.093>
7. R.J. Hinklin, B.R. Baer, S.A. Boyd, M.D. Chicarelli, K.R. Condroski, W.E. DeWolf Jr., J. Fischer, M. Frank, G.P. Hingorani, P.A. Lee, N.A. Neitzel, S.A. Pratt, A. Singh, F.X. Sullivan, T. Turner, W.C. Voegtli, E.M. Wallace, L. Williams and T.D. Aicher, Discovery and Preclinical Development of AR453588 as an Anti-diabetic Glucokinase Activator, *Bioorg. Med. Chem.*, **28**, 115232 (2019); <https://doi.org/10.1016/j.bmc.2019.115232>

8. J.A. Pfefferkorn, M. Tu, K.J. Filipski, A. Guzman-Perez, J. Bian, G.E. Aspnes, M.F. Sammons, W. Song, J.C. Li, C.S. Jones, L. Patel, T. Rasmusson, D. Zeng, K. Karki, M. Hamilton, R. Hank, K. Atkinson, J. Litchfield, R. Aiello, L. Baker, N. Barucci, P. Bourassa, F. Bourbonnais, T. D'Aquila, D.R. Derksen, M. MacDougall and A. Robertson, The Design and Synthesis of Indazole and Pyrazolopyridine Based Glucokinase Activators for the Treatment of Type 2 Diabetes Mellitus, *Bioorg. Med. Chem. Lett.*, **22**, 7100 (2012); <https://doi.org/10.1016/j.bmcl.2012.09.082>
9. K.J. Filipski, A. Guzman-Perez, J. Bian, C. Perreault, G.E. Aspnes, M.T. Didiuk, R.L. Dow, R.F. Hank, C.S. Jones, R.J. Maguire, M. Tu, D. Zeng, S. Liu, J.D. Knafels, J. Litchfield, K. Atkinson, D.R. Derksen, F. Bourbonnais, K.S. Gajiwala, M. Hickey, T.O. Johnson, P.S. Humphries and J.A. Pfefferkorn, Pyrimidone-Based Series of Glucokinase Activators with Alternative Donor–Acceptor Motif, *Bioorg. Med. Chem. Lett.*, **23**, 4571 (2013); <https://doi.org/10.1016/j.bmcl.2013.06.036>
10. R. Ragno, www.3d-qsar.com: A Web Portal that Brings 3-D QSAR to All Electronic Devices—The Py-CoMFA Web Application as Tool to Build Models from Pre-aligned Datasets, *J. Comput. Aided Mol. Des.*, **33**, 855 (2019); <https://doi.org/10.1007/s10822-019-00231-x>
11. www.3d-qsar.com
12. Y.N. Kumar, J.A. Pradeep Kiran, P.S. Kumar, S. Yeswanth, K. Kalpana, V. Koteswara Rao, P.V.G.K. Sarma and M. Bhaska, Molecular Docking Assessment of Pyridone Derivatives as Glucokinase Activators, *J. Clin. Sci. Res.*, **1**, 163 (2012).